Lethal Synergism of 2009 Pandemic H1N1 Influenza Virus and *Streptococcus pneumoniae* Coinfection Is Associated with Loss of Murine Lung Repair Responses

John C. Kash,[a] Kathie-Anne Walters,[b] A. Sally Davis,[a] Aline Sandouk,[a] Louis M. Schwartzman,[a] Brett W. Jagger,[a] Daniel S. Chertow,[a] Li Qi,[a] Rolf E. Kuestner,[b] Adrian Ozinsky,[b] and Jeffery K. Taubenberger[a]

Viral Pathogenesis and Evolution Section, Laboratory of Infectious Diseases, National Institutes of Allergy and Infectious Diseases, National Institutes of Health, Bethesda, Maryland, USA,[a] and Institute for Systems Biology, Seattle, Washington, USA[b]

ABSTRACT **Secondary bacterial infections increase disease severity of influenza virus infections and contribute greatly to increased morbidity and mortality during pandemics. To study secondary bacterial infection following influenza virus infection, mice were inoculated with sublethal doses of 2009 seasonal H1N1 virus (NIH50) or pandemic H1N1 virus (Mex09) followed by inoculation with *Streptococcus pneumoniae* 48 h later. Disease was characterized by assessment of weight loss and survival, titration of virus and bacteria by quantitative reverse transcription-PCR (qRT-PCR), histopathology, expression microarray, and immunohistochemistry. Mice inoculated with virus alone showed 100% survival for all groups. Mice inoculated with Mex09 plus *S. pneumoniae* showed severe weight loss and 100% mortality with severe alveolitis, denuded bronchiolar epithelium, and widespread expression of apoptosis marker cleaved caspase 3. In contrast, mice inoculated with NIH50 plus *S. pneumoniae* showed increased weight loss, 100% survival, and slightly enhanced lung pathology. Mex09-*S. pneumoniae* coinfection also resulted in increased *S. pneumoniae* replication in lung and bacteremia late in infection. Global gene expression profiling revealed that Mex09-*S. pneumoniae* coinfection did not induce significantly more severe inflammatory responses but featured significant loss of epithelial cell reproliferation and repair responses. Histopathological examination for cell proliferation marker MCM7 showed significant staining of airway epithelial cells in all groups except Mex09-*S. pneumoniae*-infected mice. This study demonstrates that secondary bacterial infection during 2009 H1N1 pandemic virus infection resulted in more severe disease and loss of lung repair responses than did seasonal influenza viral and bacterial coinfection. Moreover, this study provides novel insights into influenza virus and bacterial coinfection by showing correlation of lethal outcome with loss of airway basal epithelial cells and associated lung repair responses.**

IMPORTANCE **Secondary bacterial pneumonias lead to increased disease severity and have resulted in a significant percentage of deaths during influenza pandemics. To understand the biological basis for the interaction of bacterial and viral infections, mice were infected with sublethal doses of 2009 seasonal H1N1 and pandemic H1N1 viruses followed by infection with *Streptococcus pneumoniae* 48 h later. Only infection with 2009 pandemic H1N1 virus and *S. pneumoniae* resulted in severe disease with a 100% fatality rate. Analysis of the host response to infection during lethal coinfection showed a significant loss of responses associated with lung repair that was not observed in any of the other experimental groups. This group of mice also showed enhanced bacterial replication in the lung. This study reveals that the extent of lung damage during viral infection influences the severity of secondary bacterial infections and may help explain some differences in mortality during influenza pandemics.**

Received 27 July 2011 **Accepted** 11 August 2011 **Published** 20 September 2011

Citation Kash JC, et al. 2011. Lethal synergism of 2009 pandemic H1N1 influenza virus and *Streptococcus pneumoniae* coinfection is associated with loss of murine lung repair responses. mBio 2(5):e00172-11. doi:10.1128/mBio.00172-11.

Editor Keith Klugman, Emory University

Address correspondence to John C. Kash, kashj@niaid.nih.gov.

Influenza viruses can cause severe respiratory tract infections associated with secondary bacterial infections (1). The 1918 influenza virus pandemic resulted in approximately 50 million deaths worldwide (2), a majority of which were associated with secondary Gram-positive bacterial infections (3, 4). Recently, analysis of 34 autopsy cases of people who died from the 2009 H1N1 pandemic influenza virus showed that over half displayed signs of secondary bacterial infections by both postmortem lung culture and histological evaluation (5). The bacteria most frequently associated with the infections in this study were *Streptococcus pneumoniae*, *Streptococcus pyogenes*, and methicillin-resistant *Staphylococcus aureus*.

The association of primary viral influenza and secondary bacterial pneumonia has been documented since the late 19th century (3, 6–9). Proposed mechanisms include increased colonization of the upper respiratory tract and bacterial-viral synergistic copathogenesis (10–14). Influenza virus infection leads to cell death and denuding of the upper respiratory epithelium that could increase the chance of colonization by bacteria in the nasopharynx (11, 15). It has also been shown that the activity of the viral neuraminidase

(NA) protein can expose additional bacterial attachment sites (16, 17). Finally, it has been suggested that there might be a role for immunopathogenic responses due to synergistic effects of viral and bacterial infection stimulating inflammation (11).

In the present study, we investigated the effects of secondary *S. pneumoniae* infection of mice that were first inoculated with either a 2009 seasonal H1N1 (sH1N1) or a 2009 pandemic H1N1 (pH1N1) influenza virus. At equivalent inoculating doses, neither the 2009 seasonal H1N1 influenza virus A/Bethesda/NIH50 (NIH50) (18) nor the 2009 H1N1 pandemic virus A/Mexico/4108/09 (Mex09) (19) infection caused death in the absence of bacterial coinfection. Following inoculation with *S. pneumoniae*, NIH50-*S. pneumoniae*-infected mice showed only a modest increase in disease severity, but no deaths. In contrast, Mex09-*S. pneumoniae*-infected mice showed acute, severe disease with death by 4 days post-bacterial infection. Analysis of viral and bacterial replication by quantitative reverse transcription-PCR (qRT-PCR) showed that both Mex09 and NIH50 viral infection led to increased bacterial replication by 24 h post-*S. pneumoniae* inoculation, with higher levels of *S. pneumoniae* replication in Mex09-*S. pneumoniae*-infected groups. At later time points, we observed an increase in *S. pneumoniae* replication in Mex09-*S. pneumoniae*-infected groups and a reduction in *S. pneumoniae* replication in NIH50-*S. pneumoniae*-infected groups. Expression microarray analysis performed on lungs of infected mice at day 5 post-viral infection showed marked differences between NIH50 and Mex09 primary viral infections, including increased inflammatory and cell stress responses in Mex09-infected animals. The expression level of inflammatory response-related genes in Mex09-*S. pneumoniae*-infected mice was similar to that in NIH50-*S. pneumoniae*- or *S. pneumoniae*-alone-infected mice. However, there was a loss of expression of genes associated with airway epithelial cell reproliferation and lung repair in mice infected with Mex09 plus *S. pneumoniae* that could be correlated with increased detection of proapoptosis protein expression and also the loss of cell proliferation protein marker by immunohistochemical staining. There was also prominent attachment of *S. pneumoniae* to, and death of, progenitor basal epithelial cells, which play a key role in lung epithelium repair processes, in the lungs of Mex09-*S. pneumoniae*-coinfected mice. This study reveals that increased mortality due to coinfection of 2009 pandemic H1N1 virus and *S. pneumoniae* bacteria was associated with increased *S. pneumoniae* replication, death of basal epithelial cells, and loss of airway epithelial cell reproliferation not observed with 2009 seasonal H1N1 virus coinfection with *S. pneumoniae*.

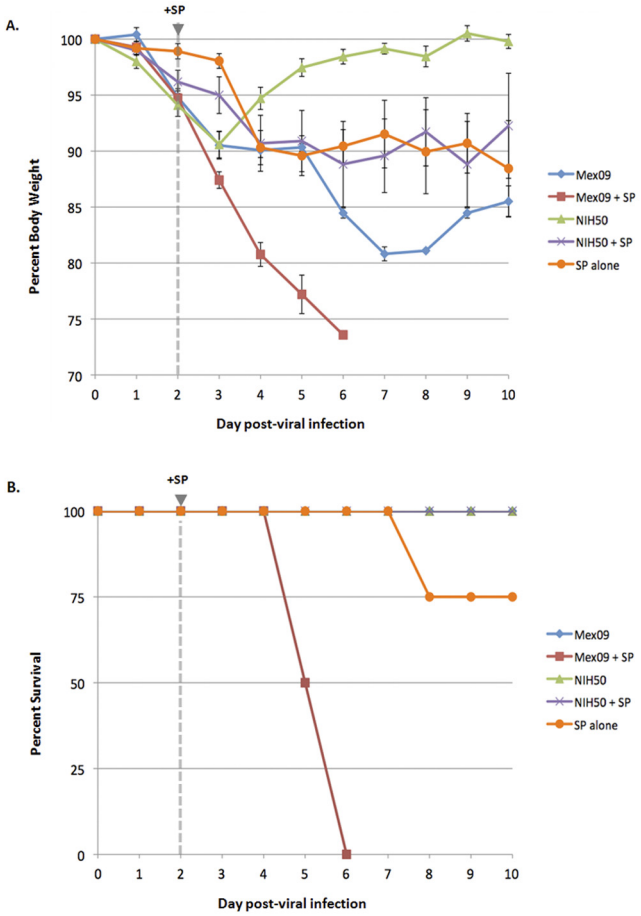

FIG 1 Weight loss and survival of mice infected with equivalent doses of 2009 pandemic H1N1 or 2009 seasonal H1N1 influenza viruses following inoculation with type III capsule *Streptococcus pneumoniae* strain. Groups of five mice were inoculated with phosphate-buffered saline or infected with 10^5 PFU of either A/Mexico/4108/09 (Mex09) or A/Bethesda/NIH50/09 (NIH50) and 48 h later were inoculated with 10^5 CFU of luciferase-expressing *Streptococcus pneumoniae* strain A66.1-*lux*. (A) Change in body weight following initial influenza virus infection. Inoculation with *S. pneumoniae* is indicated at 2 days postinfection. (B) Survival of mice following infection with influenza virus or *S. pneumoniae* or coinfection of virus and *S. pneumoniae*.

RESULTS

Outcome of coinfection is influenced by initial influenza virus. Mice inoculated with 10^5 PFU of virus alone showed mild to modest disease severity with peak weight losses of 10% and 20% for NIH50 and Mex09, respectively, with 100% survival (Fig. 1). Mice inoculated with 10^5 CFU of serotype 3 *Streptococcus pneumoniae* strain A66.1-*lux* alone displayed moderate illness with approximately 10% average weight loss and 75% survival. Mice inoculated with NIH50 followed by *S. pneumoniae* at 48 h postinfection (hpi) showed signs of more severe illness, as evidenced by increased peak weight loss, similar to *S. pneumoniae*-alone-inoculated animals, but with 100% survival. In contrast, mice coinfected with Mex09 followed by *S. pneumoniae* 48 h later showed more severe disease with dramatic weight loss and 0% survival by 6 days post-infection with virus (4 days post-infection with *S. pneumoniae*). Similar results were obtained in mice coinfected with serotype 2 *S. pneumoniae* strain D39 (data not shown). Thus, coinfection with *S. pneumoniae* in a mouse with a nonlethal dose of Mex09 infection results in uniformly lethal disease that was not observed with an identical infectious dose of NIH50.

Lethal coinfection is associated with early increased bacterial replication but not viral replication. To determine if increased viral and/or bacterial replication levels were associated with mortality, we measured influenza virus M gene expression and bacterial 16S rRNA expression by qRT-PCR (Fig. 2). Quantitation of bacterial 16S rRNA as a measurement of bacterial replication shows good correlation with CFU data (data not shown). As shown in Fig. 2A, animals inoculated with virus alone had slightly higher levels of Mex09 M gene expression than NIH50 M gene expression at days 2 to 5 postinfection that were most pronounced at days 4 to 5, consistent with results from previous studies (18). There was a similar trend of increased M gene expression in

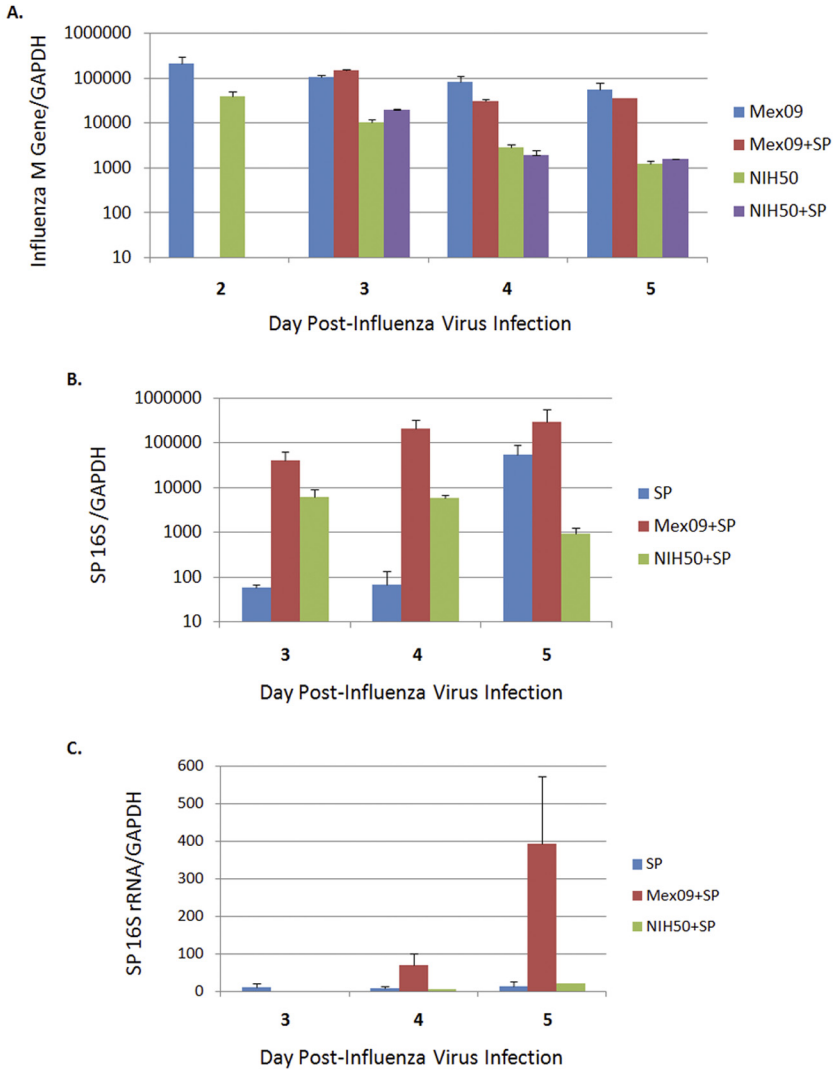

FIG 2 Replication of 2009 pandemic and seasonal H1N1 influenza virus and *Streptococcus pneumoniae* in mouse lung and spleen. (A) Expression of influenza virus M gene in lung by qRT-PCR at 2 to 5 days post-infection with influenza virus. (B) Determination of bacterial 16S rRNA by qRT-PCR from lung homogenates at 1 to 3 days post-infection with *S. pneumoniae* (3 to 5 days post-infection with influenza virus). (C) Determination of bacterial 16S rRNA by qRT-PCR from spleen homogenates at 1 to 3 days post-infection with *S. pneumoniae* (3 to 5 days post-infection with influenza virus). Data are presented as average expression values ± standard errors of the means.

Mex09-*S. pneumoniae*-infected compared to NIH50-*S. pneumoniae*-infected animals, although bacterial coinfection did not appear to result in increased viral replication of either Mex09 or NIH50. However, as shown in Fig. 2B, viral and bacterial coinfection resulted in accelerated pulmonary *S. pneumoniae* replication on days 2 to 3 compared to that in animals inoculated with *S. pneumoniae* alone. Moreover, the levels of 16S rRNA were higher for Mex09-*S. pneumoniae*-infected compared to NIH50-*S. pneumoniae*-infected animals at all times. By day 5 postinfection, animals inoculated with Mex09 plus *S. pneumoniae* and *S. pneumoniae*-alone-inoculated animals showed similar levels of *S. pneumoniae* replication while NIH50-*S. pneumoniae* coinfection resulted in decreased *S. pneumoniae* replication compared to that with *S. pneumoniae* alone. Interestingly, at day 5 postinfection, Mex09-*S. pneumoniae*-infected animals showed evidence of bacteremia with *S. pneumoniae* detection in the spleen (Fig. 2C). Together, these results indicate that enhanced bacterial replication occurred in virus-coinfected animals early after *S. pneumoniae* infection and that Mex09 coinfection resulted in higher levels of *S. pneumoniae* replication in lung and also signs of bacteremia late in infection.

Lethal coinfection is associated with more severe lung pathology. Histopathological analyses performed on animals at 5 days post-infection with NIH50 or Mex09 alone showed a range of changes compatible with an influenza viral pneumonia, including bronchitis, bronchiolitis, and alveolitis. NIH50-infected animals displayed a multifocal, mild to moderate bronchointerstitial pneumonia characterized by lymphohistiocytic bronchitis and bronchiolitis with occasional small foci of alveolitis (Fig. 3A). Influenza virus antigen was observed in the superficial respiratory epithelial cells of the bronchial and bronchiolar tree and less frequently in alveolar epithelial cells and alveolar macrophages (Fig. 3B). In contrast, lungs from Mex09-infected mice showed more severe changes with nearly diffuse bronchitis, bronchiolitis, and multifocal alveolitis (Fig. 3C). Influenza virus antigen was detected in these mice in a distribution similar to that in NIH50-infected mice (Fig. 3D).

Lungs from mice infected with NIH50 plus *S. pneumoniae* displayed a mild to moderate, multifocal, acute neutrophil-predominant bronchopneumonia predominantly at foci overlapping lesions consistent with those seen with NIH50-only infection (Fig. 3E). In contrast, lungs from mice infected with Mex09 plus *S. pneumoniae* showed a multifocal, moderate to severe, acute neutrophil-predominant bronchopneumonia admixed with a diffuse lymphohistiocytic bronchointerstitial pneumonia as described for Mex09-only infection (Fig. 3G). In contrast to NIH50-*S. pneumoniae* infection, there was a marked loss of the epithelium in bronchioles. Two of the animals also showed a multifocal bacterial pleuritis. Viral antigen distribution was similar to that seen in virus-only-infected animals (data not shown). In animals coinfected with NIH50 or Mex09 plus *S. pneumoniae*, tissue Gram staining revealed abundant bacteria both extracellularly and intracellularly within epithelial cells of the respiratory tree and in alveolar epithelial cells and alveolar macrophages (Fig. 3F and H, respectively). Pathology of *S. pneumoniae*-only-infected mice varied from normal to nearly diffuse, severe acute neutrophil-predominant pleuritis, to focal, severe acute neutrophil-predominant bronchopneumonia (data not shown).

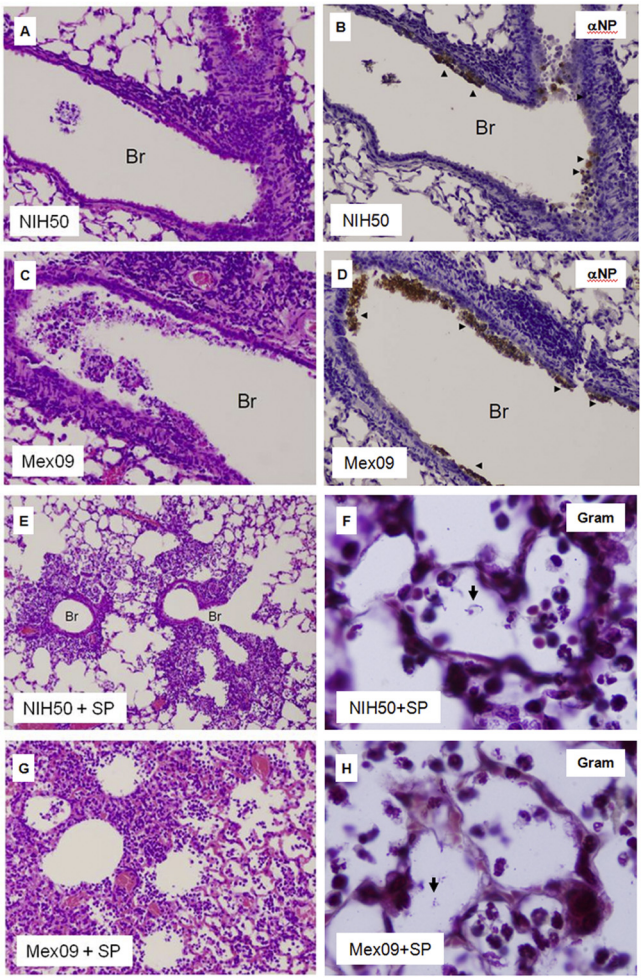

FIG 3 Lung pathology, influenza virus antigen, and Gram staining during primary infection with 2009 pandemic or 2009 seasonal H1N1 influenza viruses in the presence and absence of coinfection with *Streptococcus pneumoniae*. Lungs from infected mice (three per group) were harvested at 5 days post-infection with influenza virus (3 days post-infection with *S. pneumoniae* in coinfection groups) and were stained with hematoxylin and eosin or immunostained for influenza viral antigen (αNP). (A) Hematoxylin and eosin staining of NIH50-infected lung (original magnification, ×200); (B) immunostaining for αNP of NIH50-infected lung (original magnification, ×200); (C) hematoxylin and eosin staining of Mex09-infected lung (original magnification, ×200); (D) immunostaining for αNP of Mex09-infected lung (original magnification, ×200); (E) hematoxylin and eosin staining of NIH50-*S. pneumoniae*-infected lung (original magnification, ×40); (F) Gram staining of NIH50-*S. pneumoniae*-infected lung (original magnification, ×1,000; arrow indicates bacteria); (G) hematoxylin and eosin staining of Mex09-*S. pneumoniae*-infected lung (original magnification, ×40); (H) Gram staining of Mex09-*S. pneumoniae*-infected lung (original magnification, ×1,000; arrow indicates bacteria). Br indicates bronchus (A-D) or bronchiole (E).

Global gene expression analysis demonstrates differences in inflammatory responses and lung epithelial damage during primary infection with NIH50 or Mex09. The host transcriptional response to infection was characterized to determine whether the underlying mechanisms of the selective lethal synergy during Mex09-*S. pneumoniae* coinfection were due to differences in inflammation, activation of specific apoptotic pathways, or modification of lung epithelium. The global gene expression profiles of the individual animals are shown in Fig. 4A, with 11,247 genes showing a 2-fold-or-higher change in expression (P value, <0.01) in at least one experimental group. While in general the overall transcriptional responses did not appear dramatically different between the different infections, the grouping of experiments by the clustering algorithm suggested that the host responses were unique for each group; the most distinct response was observed in Mex09-infected animals, as evidenced by the higher number of differentially regulated genes than that in the other groups (see Fig. S1 in the supplemental material).

The expression level of genes involved in inflammation was examined to determine if there was a correlation between inflammation and infection outcome. Mex09-infected animals showed the strongest inflammatory response, as indicated by the number and level of induction of inflammatory mediators (Fig. 4B). Coinfection with NIH50 plus *S. pneumoniae* was associated with increased expression relative to infection with NIH50 alone, suggesting that *S. pneumoniae* enhanced inflammation in the context of seasonal influenza virus infection. In contrast, the expression of inflammatory mediators was actually slightly lower during Mex09-*S. pneumoniae* infection than during Mex09-alone infection. Furthermore, inflammation was comparable between Mex09-*S. pneumoniae* and NIH50-*S. pneumoniae* coinfections, suggesting that the increased mortality associated with Mex09 plus *S. pneumoniae* was not due to enhanced inflammation following bacterial infection at this time point. However, it is possible that a transient increase in inflammation occurs immediately following *S. pneumoniae* infection as has been observed in other studies (20).

Because the outcome of *S. pneumoniae* coinfection differed depending on the strain of influenza virus, it was speculated that differences in the host responses to primary viral infection may influence coinfection outcome. Analysis of variance (ANOVA) comparing NIH50- and Mex09-infected animals identified 2,171 genes as being significantly differentially expressed between the two groups (P value, <0.01; at least 2-fold difference in median expression level) (see Fig. S2A in the supplemental material). Gene ontology analysis of this group showed enrichment of genes associated with cell cycle regulation, inflammation, tissue remodeling/repair, DNA damage response, and apoptosis (Fig. 5A). The majority of apoptosis-related genes were associated with endoplasmic reticulum (ER) stress response, inflammation, and death receptor signaling. Genes associated with tissue remodeling/repair included those involved in respiratory epithelial repair (hepatocyte growth factor [HGF], keratinocyte growth factor [KGF], and extracellular membrane [ECM] components) and acute lung injury (SERPINE1). Many of these genes were more highly induced during Mex09 infection (Fig. 5B), suggesting that while both Mex09- and NIH50-infected animals recover, infection with Mex09 is associated with more extensive damage to the lung epithelium that requires more extensive tissue repair. Indeed, staining for cleaved caspase 3 (cCASP3) in the lungs of infected mice showed more abundant cCASP3 in Mex09-infected than in NIH50-infected mice (Fig. 5C and D). Most significantly, increased cCASP3 staining of basal epithelial cells was observed in the bronchiolar epithelium of mice infected with Mex09 and not with NIH50.

Lethal Mex09-*S. pneumoniae* coinfection is associated with lack of induction of lung epithelial cell proliferation and tissue repair processes. Because a significant increase in inflammatory responses did not correlate with lethal outcome of Mex09-*S. pneu-*

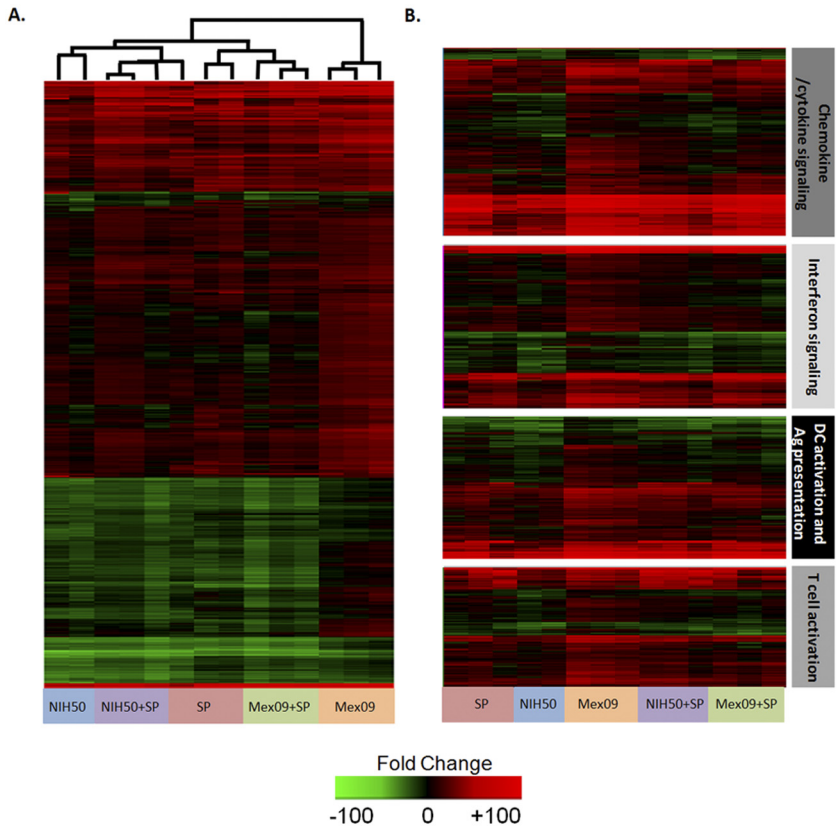

FIG 4 Host transcriptional response in the lungs of animals inoculated with influenza virus and *Streptococcus pneumoniae*. (A) Two-dimensional hierarchical clustering heat map showing the expression profiles of 11,247 sequences that are regulated (≥2-fold; *P* value, ≤0.01) in at least one experimental group. Each column represents gene expression data from an individual experiment comparing RNA from lung tissue from an infected animal isolated at 5 days postinfection relative to pooled RNA from lung tissue from mock-infected animals ($n = 9$). Genes shown in red were upregulated, genes shown in green were downregulated, and genes in black indicate no change in expression in infected animals relative to uninfected animals. (B) Expression profiles of inflammatory response genes in the lungs of infected animals. The heat map depicts genes regulated (≥2-fold; *P* value, ≤0.01) in at least 1 experiment. DC, dendritic cell; Ag, antigen.

moniae infection compared to Mex09-alone infection, ANOVA was performed to compare Mex09- and Mex09-*S. pneumoniae*-inoculated animals to identify differences in other host response pathways. The expression levels of approximately 4,000 sequences differed significantly (at least 2-fold; *P* value, <0.01) between the groups (see Fig. S2B in the supplemental material). Functional annotation analysis showed that the enriched functional group with the highest statistically significant difference was tissue remodeling/wound repair, followed by cell differentiation, inflammation, Ca^{2+} signaling, and apoptosis (Fig. 6A). In support of this, staining for cleaved caspase 3 (cCASP3) in the lungs of coinfected mice showed a greater extent of cCASP3 in Mex09-*S. pneumoniae*-infected mice (Fig. 6C); cCASP3 was not observed in NIH50-*S. pneumoniae*-infected mice (Fig. 6D). Most significantly, prominent staining of basal epithelial cells was observed in the bronchiolar epithelium of mice infected with Mex09 plus *S. pneumoniae*. The majority of the genes associated with tissue repair/remodeling and cell differentiation also showed decreased expression in the Mex09-*S. pneumoniae*-coinfected animals relative to both Mex09-infected and mock-infected animals. This suggests that secondary bacterial infection led to the loss of protective tissue reproliferation and repair processes. Mex09-*S. pneumoniae*-infected animals also showed decreased expression of pulmonary surfactant-associated protein (Sftpa1), which together with Ca^{2+} functions to lower the surface tension at the alveolar capillary interface to facilitate efficient gas exchange (21). The expression of a more comprehensive list of genes known to be involved in lung repair was examined to explore further the possibility that lack of activation of repair processes may play a role in lethal coinfection (22). The expression levels of these genes are shown in Fig. 7A, and they include key mediators of type II alveolar epithelial cell proliferation (HGF, KGF, fibroblast growth factor 10 [FGF10], epidermal growth factor [EGF], and heparin binding EGF [HB-EGF]) along with associated signaling molecules (COX-2, Akt, and mitogen-activated protein kinase [MAPK] pathways) (22). Also shown is the expression of genes associated with cell migration and ECM remodeling that are required for reestablishing basement membrane integrity (interleukins 1b, 2, 4, and 13; integrins; and matrix metalloproteinases). In general, there was a higher expression of the majority of these genes during Mex09 infection than during Mex09-*S. pneumoniae* infection, again suggesting that aspects of the repair process were absent or markedly reduced in the presence of *S. pneumoniae* coinfection. Two of the key growth factors for type II alveolar epithelial cells, HGF and KGF, show decreased expression relative even to mock infection during Mex09-*S. pneumoniae* infection. Furthermore, of the small set of genes more highly induced in Mex09-*S. pneumoniae* infection, both MMP9 and plasminogen activator inhibitor (SERPINE1) have been shown to be associated with decreased epithelial repair (23). Increased levels of SERPINE1 in bronchoalveolar lavage fluids have also been associated with increased mortality in *Pseudomonas aeruginosa*-infected patients (24). Finally, transforming growth factor β (TGF-β) levels were higher in Mex09-*S. pneumoniae* infection, and while this cytokine plays an important role in repair, inappropriate or continuous expression results in the development of fibrosis. This in turn can cause distortion of lung architecture and pulmonary hypertension (25).

Basal epithelial cells are a major source of HGF and KGF, and their destruction would be consistent with a lack of expression of these growth factors observed in Mex09-*S. pneumoniae*-infected animals. This in turn would compromise the repair of damaged lung epithelium. Immunohistochemistry to detect the cell proliferation marker MCM7 was performed to examine for differences in epithelial cell reproliferation. Prominent staining of MCM7 was detected in nuclei of basal cells in bronchioli in NIH50-, NIH50-*S. pneumoniae*-, and Mex09-infected

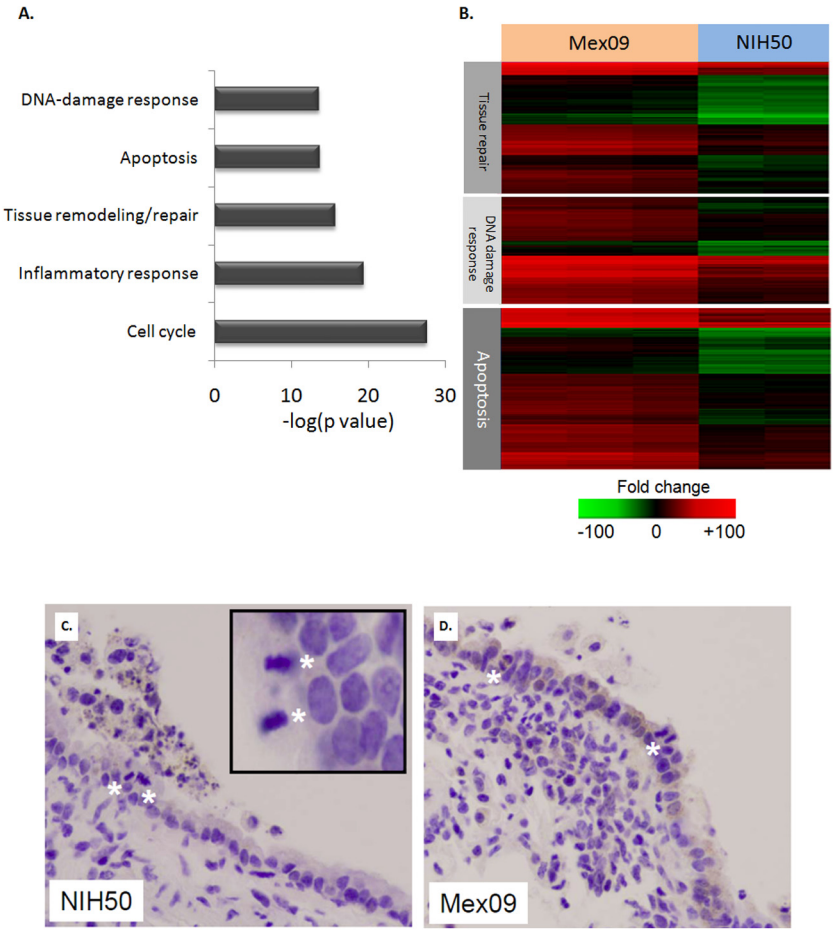

FIG 5 Differences in host responses to primary viral infection and enhanced inflammation and lung damage associated with Mex09 infection. (A) Functional annotation analysis of sequences whose expression levels differed significantly (*P* value, <0.01; ≥2-fold in expression level) between Mex09 and NIH50 infection. The graph represents only the top-five-scoring functional categories. (B) Expression profiles of a subset of the sequences from panel A. Each column represents gene expression data from an individual experiment comparing lung tissue from an infected animal to pooled tissue from mock-infected animals ($n = 9$). Genes shown in red were upregulated, genes shown in green were downregulated, and genes in black indicate no change in expression in infected animals relative to uninfected animals. (C and D) Immunohistochemical detection of cleaved caspase 3 in the lungs of virus-infected mice (original magnifications, ×200). Asterisks denote mitotic cells (inset in panel C; original magnification, ×1,000).

mouse lungs but with much less staining in Mex09-*S. pneumoniae*-infected mice, often correlating with a complete loss of epithelial cells (Fig. 7B). A more detailed analysis of Mex09-*S. pneumoniae*-infected lungs by Gram staining showed numerous *S. pneumoniae* bacteria on the few remaining basal epithelial cells, suggesting that bacterial attachment was associated with the death of basal epithelial cells (Fig. 7C). As basal epithelial cells play a key role in lung epithelium repair, including production of KGF and FGF10, their death could result in loss of airway epithelial cell reproliferative capacity.

Collectively, these data suggest that the uniform lethality of the Mex09-*S. pneumoniae* coinfection results from earlier pulmonary bacterial replication and enhanced damage to lung architecture, including death of basal epithelial cells and loss of repair and reproliferation responses, which lead to spread of the bacteria outside the lung.

DISCUSSION

Bacterial secondary infections played significant roles in the increased morbidity and mortality during past influenza virus pandemics (3). Although antibiotics have decreased to some extent the impact of secondary infections, bacterial pneumonia following influenza virus infection has continued to pose a significant threat to human health. Several mechanisms have been proposed to explain the association between primary influenza viral and secondary bacterial infections, including increased colonization, changes in airway function, increased respiratory compromise, increased inflammatory responses, and synergy between influenza viral and bacterial replication (7, 11). This study reveals that death of progenitor basal epithelial cells and loss of airway epithelial cell reproliferation and lung repair responses may also play a role in disease severity.

The upper respiratory tract contains numerous physical barriers that impede the introduction of foreign materials, including bacteria, into the lung. Damage and necrosis of epithelial cells lining the respiratory tree lead to loss of mucociliary clearance and can facilitate colonization of the lungs with bacteria present in the oronasopharynx (11). It has also been proposed that bacterial colonization of the upper respiratory tract is accelerated due to epithelial cell damage and exposure of attachment sites by viral neuraminidase (NA) activity (6, 26). In addition, inflammatory responses, including fibrin deposition, tissue repair, and regenerative processes, can result in the exposure of bacterial attachment sites. Several studies have suggested that enhanced influenza viral replication could also occur due to increased proteolytic processing of viral HA_0 protein by bacterial proteases (27). Although increased viral replication was not observed in our study, we did observe an increase in pulmonary bacterial 16S rRNA expression during Mex09-*S. pneumoniae* coinfection.

Once bacterial coinfection is established, severity of respiratory compromise can occur in response to blockage and loss of small airway function and development of exudative transmural pleuritis (11, 28). Additionally, dysregulation of immune responses can contribute to disease severity and compromise of lung function during influenza virus and bacterial coinfection (29). Our results, however, showed that activation of inflammatory responses prior to death during bacterial coinfection, as measured by gene expression, appeared to be independent of lung pathology and survival. Primary viral infection with Mex09 resulted in increased inflammatory and cell death responses that were accom-

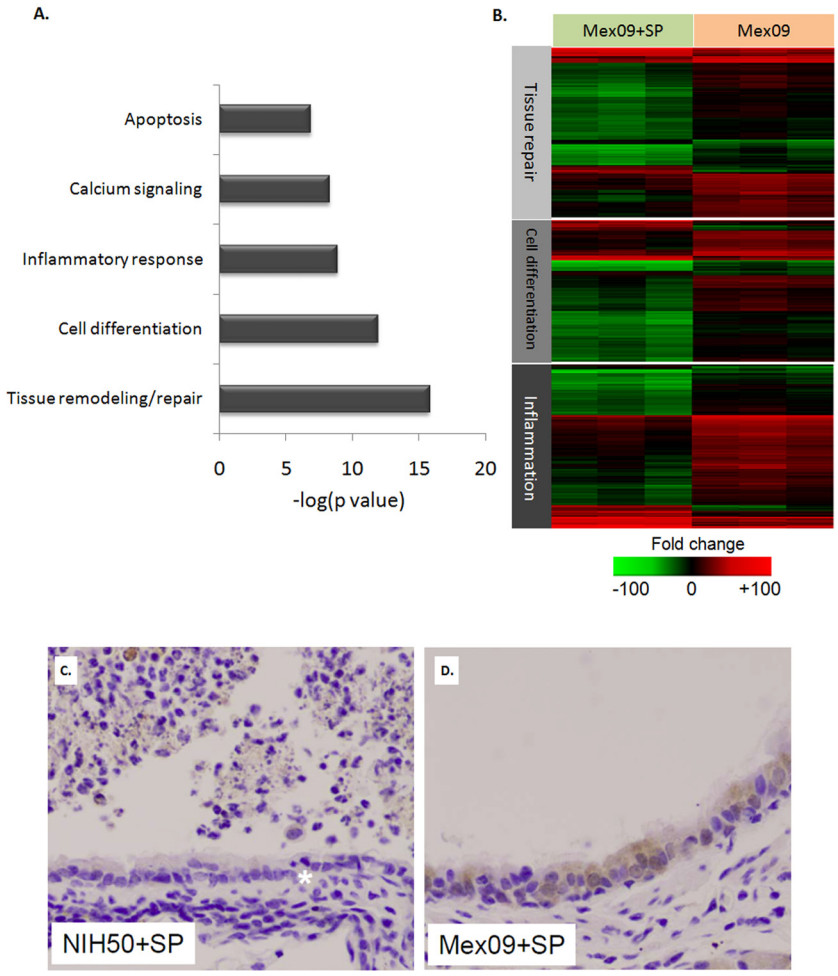

FIG 6 Coinfection with Mex09 plus *S. pneumoniae* is associated with altered cell death and tissue repair responses. (A) Functional annotation analysis of sequences whose expression levels differed significantly (*P* value, <0.01; ≥2-fold in expression level) between Mex09 and Mex09-*S. pneumoniae* infection. The graph represents only the top-five-scoring functional categories. (B) Expression profiles of a subset of the sequences from panel A. Each column represents gene expression data from an individual experiment comparing lung tissue from an infected animal to pooled tissue from mock-infected animals ($n = 9$). Genes shown in red were upregulated, genes shown in green were downregulated, and genes in black indicate no change in expression in infected animals relative to uninfected animals. (C and D) Immunohistochemical detection of cleaved caspase 3 in the lungs of bacterium-coinfected mice (original magnifications, ×200). The asterisk denotes a mitotic cell.

panied by strong lung repair and reproliferation responses compared to NIH50 primary viral infection. In contrast, animals infected with Mex09 plus *S. pneumoniae* showed slightly decreased activation of inflammatory response-related gene expression relative to Mex09-only infection but with a significant loss of lung repair responses.

Repair of lung epithelium involves several steps: proliferation and differentiation of progenitor basal epithelial cells, migration/spreading of these cells to cover the denuded areas, and resolution (22, 30). Our study suggests that a more virulent primary influenza viral infection, with increased loss of the more superficial airway epithelial cells, may lead to increased bacterial replication and attachment to the exposed basal epithelial cells and the associated loss of these critical respiratory epithelial progenitor cells (29). The lack of expression of genes encoding key growth factors normally produced by basal cells and the marked loss of basal epithelial cells observed histologically in the lungs of Mex09-*S. pneumoniae*-infected animals support this hypothesis. Loss of basal epithelial cells would preclude the reestablishment of the normal airway epithelium, resulting in increased and sustained respiratory compromise and death (30). Increased lung damage and lack of lung repair processes could also lead to loss of tissue integrity and spread of bacteria outside the lung. This is supported by the bacteremia observed in the Mex09-*S. pneumoniae*-infected animals.

The association between failure to restore lung epithelium and lethality of coinfections also raises the possibility of therapeutically targeting these repair pathways, such as treatment with exogenous KGF, which has been shown to have a protective effect in a variety of lung injury models (31). In combination with antibiotic and antiviral therapies, treatments that stimulate lung repair responses could be beneficial in improving survival.

The present study has demonstrated that outcome of influenza virus and bacterial coinfection correlated with the pathogenicity of the primary viral infection, enhanced bacterial replication, and the extent of lung repair required for survival. Increased loss of superficial respiratory epithelial cells during a more pathogenic viral infection led to exposure and subsequent death of progenitor basal epithelial cells by bacterial infection, resulting in a loss of critical respiratory epithelial cell reproliferation and lung repair processes that also likely contributed to the development of late-stage bacteremia. Thus, the severity of bacterial pneumonia resulting from enhanced lung damage from the primary viral infection, and the amount of repair necessary for recovery, may be an intrinsic measure of influenza virus pathogenicity and may help explain differences in the numbers of bacterial pneumonia-associated deaths during influenza pandemics.

MATERIALS AND METHODS

Viruses and bacteria. A/Mexico/4108/09 (H1N1; Mex09) was provided by Heinz Feldmann, NIH/NIAID (Hamilton, MT). A/Bethesda/NIH50/2009 (H1N1; NIH50) was isolated from patients at the NIH Clinical Center (protocol 07-I-0229) (18). *Streptococcus pneumoniae* D39 (serotype 2; Xen7) and *Streptococcus pneumoniae* A66.1 (serotype 3; Xen10) were purchased from Caliper Life Sciences (Alameda, CA).

Growth and titration of bacteria and viruses. Viruses were passaged on MDCK cells in the presence of 1.0 μg/ml TPCK (tolylsulfonyl phenylalanyl chloromethyl ketone)-treated trypsin in Dulbecco's modified Eagle medium (DMEM), and virus titers were determined as described in reference 32. Virus titers were calculated according to the method of Reed

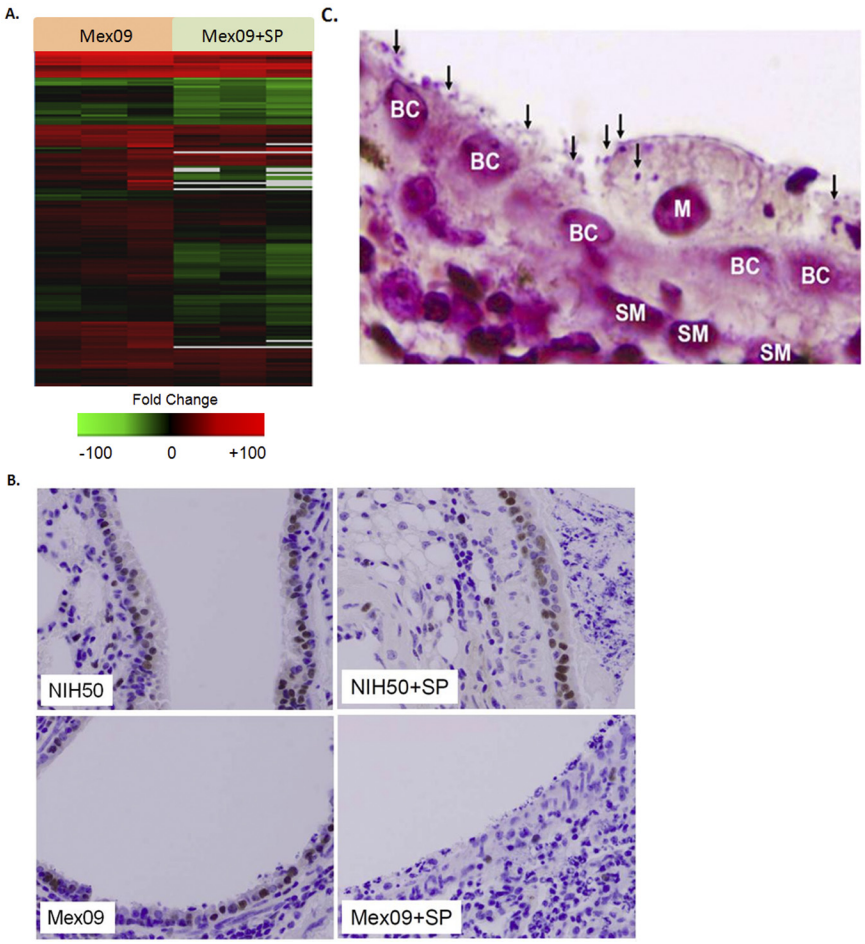

FIG 7 Mex09-*S. pneumoniae* infection is associated with loss of basal cells and absence of reproliferation of airway epithelial cells. (A) Heat map showing tissue repair pathway gene expression data where each column represents data from an individual experiment comparing lung tissue from an infected animal to pooled tissue from mock-infected animals ($n = 9$). Genes shown in red were upregulated, genes shown in green were downregulated, and genes in black indicate no change in expression in infected animals relative to uninfected animals. (B) Immunohistochemistry for presence of the cell proliferation marker MCM7 in lungs of infected mice (original magnifications, ×200). (C) Presence of *S. pneumoniae* bacteria (arrows) on remaining basal epithelial cells (nuclei labeled BC) and a macrophage (M) during Mex09-*S. pneumoniae* coinfection; smooth muscle cells below the basement membrane are labeled SM (original magnification, ×1,000).

and Muench (33). All work was performed in an enhanced biosafety level 3 (BSL-3) laboratory at the National Institutes of Health (NIH). *Streptococcus pneumoniae* was cultured in brain and heart-infused medium (BHI) and grown on BHI agar plates supplemented with 5% sheep erythrocytes according to the manufacturer's directions.

Mouse infection studies. Groups of five 8- to 10-week-old female BALB/c mice (Jackson Labs, Bar Harbor, ME) were lightly anesthetized in a chamber with isoflurane supplemented with O_2 (1.5 liters/min) and intranasally inoculated with 10^5 PFU of Mex09 or NIH50 in a total volume of 50 μl. At 48 h later, mice were inoculated intranasally with 10^5 CFU of *Streptococcus pneumoniae*. Body weights were measured daily, and mice were humanely euthanized if they lost more than 25% of their starting body weight. Lungs were collected for RNA isolation at days 2 through 5 post-influenza virus infection (3 days post-bacterial infection) and for pathology at day 5. For each virus and time point, lungs from 3 animals were collected for microarray: 3 lungs on days 2 to 4 and 6 lungs on day 5 for viral and bacterial titration by qRT-PCR and from 3 animals for pathology. Lungs collected for pathology were inflated with 10% neutral buffered formalin at time of isolation to prevent atelectasis. All experimental animal work was performed in an enhanced animal BSL-3 (ABSL-3) laboratory at the National Institutes of Health (NIH) following approval of animal safety protocols by the NIH Animal Care and Use Committee.

RNA isolation and expression microarray analysis. Total RNA was isolated from lung by homogenization (10% [wt/vol]) in Trizol (Invitrogen, Carlsbad, CA) followed by chloroform extraction and isopropanol precipitation. RNA quality was assessed using a BioAnalyzer (Agilent Technologies). Gene expression profiling experiments were performed using Agilent Mouse Whole Genome 44K microarrays. Fluorescent probes were prepared using the Agilent QuickAmp labeling kit according to the manufacturer's instructions. For each microarray experiment, mRNA isolated from the lungs of an individual animal inoculated with either *S. pneumoniae* alone, influenza virus alone, or influenza virus followed by *S. pneumoniae* was compared to a pool of mRNA isolated from the lungs of mock animals ($n = 9$). Each RNA sample (2 to 3 biological replicates per condition) was labeled and hybridized to individual arrays. Spot quantitation was performed using Agilent's Feature Extractor software, and all data were then entered into a custom-designed database, SlimArray, and then uploaded into GeneData Analyst 2.1 (GeneData) and Spotfire Decision Suite 8.1 (Spotfire, Somerville, MA). Data normalization was performed in GeneData Analyst using central tendency followed by relative normalization using pooled RNA from mock-infected mouse lung as reference. Metacore version 6.3 and Entrez Gene (http://www.ncbi.nlm.nih.gov/sites) were used for gene ontology and pathway analysis.

Quantitative RT-PCR. Quantitative real-time PCR was used to estimate bacterial and viral loads in lung and spleen tissue. Reverse transcription of total RNA was performed with primers specific for either *Streptococcus pneumoniae* 16S rRNA or influenza virus matrix 1 (M) gene using the Superscript III first-strand cDNA synthesis kit (Invitrogen, Carlsbad, CA). TaqMan primers and probe were designed to the *Streptococcus pneumoniae* 16S rRNA gene using Primer Express 3.0 software (Applied Biosystems, Foster City, CA), generating the following primers and probe: forward, 5′ GGTGACGGC AAGCTAATCTCTT 3′; reverse, 5′ AGGCGAGTTGCAGCCTACAA 3′; and probe, 5′ AAGCCAGTCTCAGTTCG 3′. Primers and probe were designed to a highly conserved region among influenza A virus matrix protein 1 genes, generating the following primers and probe: forward, 5′ TCAGGCCCCCTCAAAGCCGAGAT 3′; reverse, 5′ CGTCTACGCTG CAGTCCTC 3′; probe, 5′ TTTGTGTTCACGCTCACCGTGCCCA 3′. Real-time PCR was performed using an ABI 7900HT Fast real-time PCR system. Each target was run in duplicate with TaqMan 2× PCR Universal Master Mix and a 5-μl total reaction volume. Endogenous control primer and probe sets for relative quantification to glyceraldehyde-3-phosphate dehydrogenase (GAPDH) mRNA were obtained from Applied Biosystems, Foster City, CA. Quantification of each gene's threshold cycle (Ct) was graphed relative to that of the calibrator, mouse GAPDH (ABI catalog

no. 4352932-0708015) and mammalian 18S rRNA (ABI catalog no. HS99999901_s1), and two-tailed *P* values were calculated using an unpaired *t* test.

Pathology and immunohistochemistry. Tissue samples were dehydrated and embedded in paraffin, and 5-μm sections on positively charged slides were stained with hematoxylin and eosin for histopathologic examination. Gram staining was performed with the Brown and Hopps method (5). For immunohistochemical staining, primary antibody for influenza virus antigen distribution was a goat polyclonal anti-influenza A virus H1N1 antibody (OBT1551; AbD Serotec, Raleigh, NC) at a dilution of 1:500. The antibody was revealed and visualized per vendor instructions with an avidin-biotin-peroxidase complex (ABC) technique (Vectastain ABC kit PK-4005; Vector Labs, Burlingame, CA) and 3,3′-diaminobenzidine chromogen (DAB). A hematoxylin counterstain was added. The primary antibody for detecting apoptosis distribution was a cleaved caspase 3 (Asp175) rabbit monoclonal antibody (5A1E; Cell Signaling Technology, Danvers, MA), and the primary antibody for detecting proliferation was an MCM7 (EP1974Y) rabbit monoclonal antibody (ab52489; Abcam, Cambridge, MA), both at a dilution of 1:200. Their immunohistochemical protocols included a 15-min steam antigen retrieval with pH 6 citrate buffer (Target Retrieval solution S1699; Dako, Carpinteria, CA), primary antibody dilution in background reducing diluent (S3022; Dako), ABC technique (Vectastain ABC kit PK-6160), visualization with DAB, and hematoxylin counterstaining.

ACKNOWLEDGMENTS

This work was supported by the Intramural Research Program of the NIH and the NIAID. K.-A.W., R.E.K., and A.O. were supported by Defense Threat Reduction Agency contract HDTRA-1-08-C-0023.

We thank David Morens at NIAID/NIH for helpful discussions. Animal care and immunohistochemistry were performed by the Comparative Medicine Branch, NIH/NIAID.

SUPPLEMENTAL MATERIAL

Supplemental material for this article may be found at http://mbio.asm.org/lookup/suppl/doi:10.1128/mBio.00172-11/-/DCSupplemental.

Figure S1, PDF file, 0.2 MB.

Figure S2, PDF file, 0.6 MB.

REFERENCES

1. **Kuiken T, Taubenberger JK.** 2008. Pathology of human influenza revisited. Vaccine **26**(Suppl. 4):D59–D66.
2. **Johnson NP, Mueller J.** 2002. Updating the accounts: global mortality of the 1918–1920 "Spanish" influenza pandemic. Bull. Hist. Med. **76**: 105–115.
3. **Morens DM, Taubenberger JK, Fauci AS.** 2008. Predominant role of bacterial pneumonia as a cause of death in pandemic influenza: implications for pandemic influenza preparedness. J. Infect. Dis. **198**:962–970.
4. **Klugman KP, Astley CM, Lipsitch M.** 2009. Time from illness onset to death, 1918 influenza and pneumococcal pneumonia. Emerg. Infect. Dis. **15**:346–347.
5. **Gill JR, et al.** 2010. Pulmonary pathologic findings of fatal 2009 pandemic influenza A/H1N1 viral infections. Arch. Pathol. Lab. Med. **134**:235–243.
6. **DeLeo FR, Musser JM.** 2010. Axis of coinfection evil. J. Infect. Dis. **201**:488–490.
7. **Hartshorn KL.** 2010. New look at an old problem: bacterial superinfection after influenza. Am. J. Pathol. **176**:536–539.
8. **Hussell T, Williams A.** 2004. Menage a trois of bacterial and viral pulmonary pathogens delivers coup de grace to the lung. Clin. Exp. Immunol. **137**:8–11.
9. **Palacios G, et al.** 2009. *Streptococcus pneumoniae* coinfection is correlated with the severity of H1N1 pandemic influenza. PLoS One **4**:e8540.
10. **McCullers JA.** 2008. Planning for an influenza pandemic: thinking beyond the virus. J. Infect. Dis. **198**:945–947.
11. **McCullers JA.** 2006. Insights into the interaction between influenza virus and pneumococcus. Clin. Microbiol. Rev. **19**:571–582.
12. **Madhi SA, Schoub B, Klugman KP.** 2008. Interaction between influenza virus and *Streptococcus pneumoniae* in severe pneumonia. Expert Rev. Respir. Med. **2**:663–672.
13. **Klugman KP, Chien YW, Madhi SA.** 2009. Pneumococcal pneumonia and influenza: a deadly combination. Vaccine **27**(Suppl. 3):C9–C14.
14. **Takase H, et al.** 1999. Facilitated expansion of pneumococcal colonization from the nose to the lower respiratory tract in mice preinfected with influenza virus. Microbiol. Immunol. **43**:905–907.
15. **McCullers JA, et al.** 2010. Influenza enhances susceptibility to natural acquisition of and disease due to *Streptococcus pneumoniae* in ferrets. J. Infect. Dis. **202**:1287–1295.
16. **Ramphal R, et al.** 1980. Adherence of *Pseudomonas aeruginosa* to tracheal cells injured by influenza infection or by endotracheal intubation. Infect. Immun. **27**:614–619.
17. **McCullers JA, Rehg JE.** 2002. Lethal synergism between influenza virus and *Streptococcus pneumoniae*: characterization of a mouse model and the role of platelet-activating factor receptor. J. Infect. Dis. **186**:341–350.
18. **Kash JC, et al.** 2010. Prior infection with classical swine H1N1 influenza viruses is associated with protective immunity to the 2009 pandemic H1N1 virus. Influenza Other Respi. Viruses **4**:121–127.
19. **Safronetz D, et al.** 2011. Pandemic swine-origin H1N1 influenza A virus isolates show heterogeneous virulence in macaques. J. Virol. **85**: 1214–1223.
20. **Smith MW, Schmidt JE, Rehg JE, Orihuela CJ, McCullers JA.** 2007. Induction of pro- and anti-inflammatory molecules in a mouse model of pneumococcal pneumonia after influenza. Comp. Med. **57**:82–89.
21. **Walther FJ, et al.** 2007. Hydrophobic surfactant proteins and their analogues. Neonatology **91**:303–310.
22. **Crosby LM, Waters CM.** 2010. Epithelial repair mechanisms in the lung. Am. J. Physiol. Lung Cell. Mol. Physiol. **298**:L715–L731.
23. **Lazar MH, et al.** 2004. Plasminogen activator inhibitor-1 impairs alveolar epithelial repair by binding to vitronectin. Am. J. Respir. Cell Mol. Biol. **31**:672–678.
24. **Song Y, et al.** 2007. Increased plasminogen activator inhibitor-1 concentrations in bronchoalveolar lavage fluids are associated with increased mortality in a cohort of patients with *Pseudomonas aeruginosa*. Anesthesiology **106**:252–261.
25. **Wallace MJ, et al.** 2006. Role of platelet-derived growth factor-B, vascular endothelial growth factor, insulin-like growth factor-II, mitogen-activated protein kinase and transforming growth factor-beta1 in expansion-induced lung growth in fetal sheep. Reprod. Fertil. Dev. **18**: 655–665.
26. **McCullers JA, Bartmess KC.** 2003. Role of neuraminidase in lethal synergism between influenza virus and *Streptococcus pneumoniae*. J. Infect. Dis. **187**:1000–1009.
27. **Tashiro M, et al.** 1987. Role of Staphylococcus protease in the development of influenza pneumonia. Nature **325**:536–537.
28. **Kostrzewska K, Massalski W, Narbutowicz B, Zielinski W.** 1974. Pulmonary staphylococcal complications in patients during the influenza epidemic in 1971–1972. Mater. Med. Pol. **6**:207–212.
29. **Ballinger MN, Standiford TJ.** 2010. Postinfluenza bacterial pneumonia: host defenses gone awry. J. Interferon Cytokine Res. **30**:643–652.
30. **Reynolds SD, et al.** 2004. Airway injury in lung disease pathophysiology: selective depletion of airway stem and progenitor cell pools potentiates lung inflammation and alveolar dysfunction. Am. J. Physiol. Lung Cell. Mol. Physiol. **287**:L1256–L1265.
31. **Ware LB, Matthay MA.** 2002. Keratinocyte and hepatocyte growth factors in the lung: roles in lung development, inflammation, and repair. Am. J. Physiol. Lung Cell. Mol. Physiol. **282**:L924–L940.
32. **Qi L, et al.** 2009. Role of sialic acid binding specificity of the 1918 influenza virus hemagglutinin protein in virulence and pathogenesis for mice. J. Virol. **83**:3754–3761.
33. **Reed LJ, Muench H.** 1938. A simple method of estimating fifty percent endpoints. Am. J. Hyg. **27**:493–497.